^{13}C Magic Angle Spinning NMR Characterization of the Functionally Asymmetric Q_A Binding in *Rhodobacter sphaeroides* R26 Photosynthetic Reaction Centers Using Site-Specific ^{13}C-Labeled Ubiquinone-10†

W. B. S. van Liemt,‡ G. J. Boender,‡ P. Gast,§ A. J. Hoff,§ J. Lugtenburg,‡ and H. J. M. de Groot*,‡

Leiden Institute of Chemistry, Gorlaeus Laboratories, and Department of Biophysics, Huygens Laboratorium, Leiden University, P.O. Box 9502, 2300 RA Leiden, The Netherlands

Received January 6, 1995; Revised Manuscript Received June 2, 1995⊗

ABSTRACT: Photosynthetic reaction centers (RCs) of *Rhodobacter sphaeroides* R26 were reconstituted at the Q_A site with ubiquinone-10, selectively ^{13}C-enriched on positions 1, 2, 3, 4, and 3-Me (IUPAC numbering). RCs dispersed in LDAO detergent were studied with ^{13}C CP/MAS NMR spectroscopy at temperatures between 180 and 240 K, while RCs precipitated by removal of the detergent were investigated at ambient temperature and at temperatures down to 180 K. Electrostatic charge differences in Q_A induced by polarization from the protein are less than 0.02 electronic equivalent for any of the labeled positions. This includes the 4-carbonyl, which is therefore not significantly polarized by an electrostatic binding interaction with the protein. The Q_A site is slightly heterogeneous on the scale of the NMR as the observed line widths of the labels are between 150 and 300 Hz and inhomogeneous broadening is observed for the signals of positions 1, 2, and 3 upon cooling. This contrasts with earlier MAS observations for labels in the vicinity of the special pair. The chemical shifts are 184, 144, and 137 ppm for the labels at positions 1, 2, 3, and 12 ppm for the 3-methyl ^{13}C. For the 4-carbonyl only at sample temperatures below ~255 K a CP/MAS response can be observed at 183 ppm. The principal components of the chemical shift tensors for the ring labels in Q_A were estimated using difference spectroscopy. Although the asymmetry of the anisotropy of the 4-^{13}C signal from Q_A is only moderately different from the anisotropy of the 4 position in crystalline UQ_{10}, it is concluded that the NMR is compatible with a decrease of the 4 C=O bond order upon binding to the protein. The temperature-dependent asymmetry between the two carbonyls in Q_A indicates that the putative strong interaction with the protein at position 4 involves dynamic character, which may be of importance to the specific Q_A redox chemistry.

The photosynthetic RC[1] of *Rhodobacter (Rb.) sphaeroides* R26 is a transmembrane protein complex that consists of three polypeptide chains (L, M, and H) and nine cofactors: two ubiquinones-10, four bacteriochlorophylls, two bacteriopheophytins, and one non-heme Fe^{2+}. The cofactors form two branches, designated A and B, with a nearly 2-fold symmetry (Rees et al., 1989; Chang et al., 1991; Ermler et al., 1994). The ubiquinone residing in the A branch is denoted by Q_A and is very tightly bound. It permanently occupies the reaction center during the photochemistry.

Upon illumination of the protein complex an electron is transported from a bacteriochlorophyll pair (P) at the periplasmic side of the membrane to the primary quinone Q_A [for a review, see, e.g., Bixon et al., (1991)]. Interestingly, Q_A temporarily takes on only one electron under physiological conditions, thereby reaching the semiquinone state (Slooten, 1972). This is rather remarkable, as quinones generally undergo two-step reduction to the corresponding quinoles (Morrison et al., 1982). Therefore, specific protein−cofactor interactions should be responsible for the Q_A redox properties. In addition, the tight binding of Q_A in the RC can also be attributed to interactions with the protein environment.

Protein−Q_A interactions have been the subject of extensive investigations. For instance, at an early stage UV/Vis spectroscopy has been used to identify ubiquinone as the primary electron acceptor and to determine the protonation state of the semiquinone (Slooten, 1972; Wraight, 1979; Verméglio, 1982). In the X-ray structures of the Q_A binding site, the UQ_{10} carbonyls have different distances to possible protein hydrogen-bond donors, indicating a functional asymmetry between these positions (Allen et al., 1987; Chang et al., 1991; Ermler et al., 1994). Functional asymmetry also transpired from FTIR studies on the Q_A binding site and was inferred from the examination of the binding of model compounds in the Q_A site (Breton et al., 1994a,b; Brudler et al., 1994; Gunner et al., 1985; Warncke & Dutton, 1993). In addition, from ENDOR measurements and from recent Q-band EPR spectroscopy on $Q_A^{\bullet-}$, a pronounced asymmetry between both carbonyl positions in the semiquinone state was observed (Lubitz et al., 1985; Feher et al., 1985; Van den Brink et al., 1994).

† This research was supported by the Netherlands Foundations for Biophysical and Chemical Research and financed by the Netherlands Organisation for Scientific Research (NWO). P.G and H.J.M.d.G. have received a research career development fellowship from the Koninklijke Nederlandse Academie van Wetenschappen (Royal Dutch Academy of Sciences).

* To whom correspondence should be addressed.

‡ Gorlaeus Laboratories.

§ Huygens Laboratory.

⊗ Abstract published in *Advance ACS Abstracts,* July 15, 1995.

[1] Abbreviations: CP, cross-polarization; CSA, chemical shift anisotropy; DQ_0, duroquinone; FWHM, full width at half-maximum; LDAO, *N,N*-dimethyldodecylamine-*N*-oxide; MAS, magic angle spinning; NMR, nuclear magnetic resonance; Q_0, benzoquinone; RC, reaction center; RT, room temperature; TMS, tetramethylsilane; UQ_{10}, ubiquinone-10.

0006-2960/95/0434-10229$09.00/0

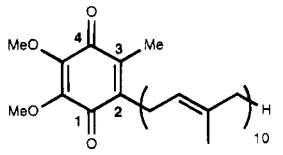

FIGURE 1: Structure of ubiquinone-10. The ^{13}C-labeled positions are indicated following the IUPAC numbering scheme.

In an attempt to investigate the molecular mechanism of the asymmetric binding of Q_A in more detail, we present the first ^{13}C CP/MAS NMR study on *Rb. sphaeroides* R26 RCs reconstituted at the Q_A site with selectively labeled ubiquinone-10. An apolar Q_A binding site transpires. The most important finding is a temperature-dependent asymmetry, since the CP/MAS signal of carbonyl 4 is not detectable at temperatures $T \geq 255$ K, contrary to the signals from the other labeled positions, including the opposite carbonyl 1. This may be interpreted as an indication that the Q_A binding involves dynamic character.

MATERIALS AND METHODS

Cells of *Rb. sphaeroides* R26 were grown in large quantities, and the RCs were purified as described by Feher and Okamura (1978). Site-specific selective labeling with ^{13}C of ubiquinone-10 [IUPAC name: 5,6-dimethoxy-3-methyl-2-[(All-E)-3′,7′11′,15′,19′,23′,27′,31′,35′,39′-decamethyl-2″,6′,10′,14′,18′,22′,26′,30′,34′,38′-tetracontadecaenyl]cyclohexa-2,5-dien-1,4-dione] is described elsewhere (Van Liemt et al., 1994). The labeled positions are indicated in Figure 1. Q_A reconstitution was performed in subdued light according to the method originally described by Okamura et al. (1975). Labeled UQ_{10} was dissolved in 0.1 mL of hexane (~20 mg/mL) and was added to 1 mL of a solution of 10 mM Tris buffer, 1 mM EDTA, and 1% Triton X-100, pH 8.0. The solution was stirred and then gently heated to 70−80 °C to evaporate the hexane and to allow the uptake of ubiquinone by the micellar buffer solution. This was then added to a suspension of Q_A-depleted R26 reaction centers in a molar ratio of about 1.5 such that the final Triton X-100 concentration was ~0.1%. The relative amount of reconstituted RCs was determined by monitoring $D^+Q_A^-$ formation after illumination. In all cases, a 95% Q_A regeneration was observed within 20 min.

After reconstitution, the RCs were loaded on a DEAE Sephacel column, which was equilibrated with 10 mM Tris buffer/0.1% LDAO and 1 mM EDTA, pH 8.0. The column was washed with 10 mM Tris buffer/0.1% LDAO and 1 mM EDTA to remove the Triton and the excess quinone. The RCs were subsequently removed from the column using 0.5 M NaCl. With this procedure the Q_B site was found to be depleted to >95%.

For the NMR experiments on frozen solutions of detergent-solubilized RCs, samples were dialyzed against Tris/LDAO to remove the excess NaCl. The solution was concentrated using a 100 kDa filter (Amicon, Ca.).

Precipitated RCs were obtained by dialyzing overnight another newly grown and reconstituted batch of LDAO-solubilized protein complexes against a suspension of Bio-Beads SM2 (Bio-Rad) (Hellingwerf, 1987; Gast et al., 1994). The reaction centers were pelleted at 2000*g* for 15 min in a swing out centrifuge (Sorvall GLC-1). Subsequently, the pellets were washed twice with 10 μM Tris buffer to minimize the dielectric susceptibility of the NMR sample. Finally, the RCs were pelleted in a centrifuge for 24 h at 300000*g*. For the difference spectroscopy, one batch of Q_A-depleted RCs was prepared for incorporation with all five differently labeled ubiquinones.

100 MHz ^{13}C CP/MAS NMR experiments were performed with an MSL-400 NMR spectrometer using a 4 mm MAS probe (Bruker, Karlsruhe, Germany). The low-temperature data were acquired after freezing the sample in the rotor with liquid nitrogen cooled bearing gas (Fischer et al., 1992). The bearing gas temperature T_B was measured just before entry of the gas into the spinner assembly. The sample temperature is slightly higher and can be approximated by $T \sim 0.86T_B + 50$ K, which is accurate to about 5 K. During the NMR experiments the sample was kept in a closed container and was shielded from the light. The spinning rate around the magic angle was stabilized with a spinning speed controller constructed in our laboratory (de Groot et al., 1988). The spectra were accumulated in 1024 channels with proton decoupling during aquisition. The 90° pulse lengths were ~4 μs. Data were collected with a recycle delay time of 1s and a sweep width of 50 kHz. The CP/MAS spectra that were used for the anisotropy analysis were recorded with a variable amplitude CP sequence (Peersen et al., 1993). All spectra are referenced to tetramethylsilane, using one of the prominent LDAO signals at 14.4 or 29.9 ppm for internal calibration. Exponential apodization was applied to the data before Fourier transformation and quoted line widths have been obtained from the spectra by subtracting the linebroadening from the apparent line widths. All spectra were recorded with 10 μs dead time, and first-order phase corrections were always kept at the same value of 48°. With this procedure, the absolute error in the chemical shift is ~0.2 ppm (Fischer et al., 1992).

The chemical shift tensors are represented in terms of the anisotropy parameter $\delta = \gamma B_0(\sigma_{zz} - \sigma_i)$, and the asymmetry parameter $\eta = (\sigma_{xx} - \sigma_{yy})/(\sigma_{zz} - \sigma_i)$, where the σ_{xx}, σ_{yy}, and σ_{zz} are the principal values of the tensor, arranged according to $|\sigma_{zz} - \sigma_i| \geq |\sigma_{xx} - \sigma_i| \geq |\sigma_{yy} - \sigma_i|$, yielding $0 \leq \eta \leq 1$, with δ sign reversal at maximum asymmetry $\eta = 1$. Chemical shift anisotropies were calculated with the Herzfeld−Berger Method (Herzfeld & Berger, 1980) or the procedures described by Munowitz and Griffin (1982), using the CERN (Geneva, Switzerland) MINUIT fitting package (de Groot et al., 1991).

Signal intensities $I(\tau_{cp})$ were measured as a function of cross-polarization time τ_{cp} and fitted to the double-exponential function (Mehring, 1983)

$$I(\tau_{cp}) = \frac{I_0}{T_{CH}} \frac{\left(\exp\frac{-\tau_{cp}}{T_{1\varrho}^H}\right) - \left(\exp\frac{-\tau_{cp}}{T_{CH}}\right)}{\frac{1}{T_{CH}} - \frac{1}{T_{1\varrho}^H}} \quad (1)$$

In this expression the I_0 sets the amplitude, T_{CH} is the characteristic polarization transfer time associated with the $^{13}C-^1H$ dipolar coupling, and $T_{1\varrho}^H$ is the longitudinal proton relaxation time in the rotating frame, i.e. under spin-lock conditions.

RESULTS

Figure 2 shows proton-decoupled ^{13}C CP/MAS data for two reconstituted [1-^{13}C]Q_A *Rb. sphaeroides* R26 RC samples.

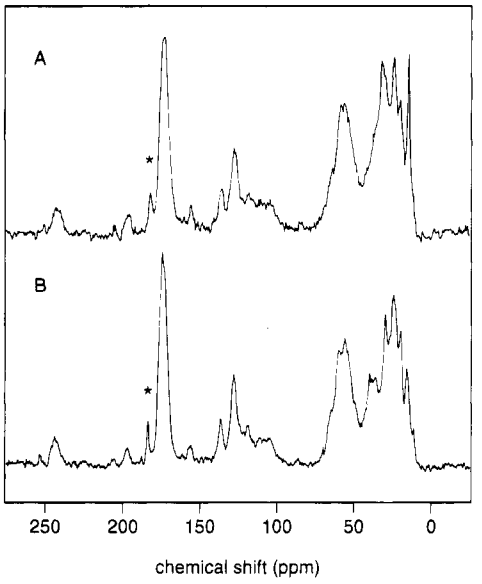

FIGURE 2: Proton-decoupled ^{13}C CP/MAS spectra of *Rb. sphaeroides* R26 RCs, reconstituted with [1-^{13}C]UQ_{10} in the Q_A site. Data were collected with a spinning speed of $\omega_r/2\pi = 7.00$ kHz from a frozen sample of detergent-solubilized RCs (A) and from a precipitated sample at ambient temperature (B).

The data in Figure 2A were collected from a detergent-solubilized sample at a temperature of 210 K, while the data in Figure 2B were obtained at room temperature from a precipitated sample. Both spectra were recorded with a spinning speed of $\omega_r/2\pi = 7.00$ kHz. The MAS NMR signal typically constitutes a sharp centerband at the isotropic chemical shift, together with a set of rotational sidebands at multiple integrals of the spinning speed, with respect to the center band. At the relatively high spinning speed of 7.00 kHz the side bands are largely absent. Three different spectral regions can be identified. Between 0 and 75 ppm, natural abundance background signals from the aliphatic carbon atoms are observed, while the aromatic and vinylic ^{13}C nuclei resonate in the 100−150 ppm range. The detergent-solubilized samples give rise to additional signals in the aliphatic region from the LDAO (Fischer et al., 1992). In each spectrum a large signal from the peptide carbonyls is visible at 173 ppm, with a weaker spinning side band at 243 ppm. The signals from the 1-^{13}C-labeled Q_A are clearly visible and are indicated with asterisks.

The detergent solubilized and precipitated samples were compared at various temperatures down to 180 K. In Figure 3A the aromatic and carbonylic responses of a detergent-solubilized 1-^{13}C Q_A sample at a temperature of 210 K are displayed. Comparison with data recorded at 190 K (Figure 3C) for the precipitated [1-^{13}C]Q_A sample shows that both preparations yield highly similar NMR responses. At room temperature the 1-^{13}C signal is shifted by ~2 ppm downfield, and its line width decreases by ~50 Hz (Figure 3B).

In Figure 3D the aromatic and carbonylic region of the [4-^{13}C]Q_A detergent solubilized sample recorded at 190 K is displayed, while the Figure 3 panels E and F show the same region of the spectrum for a precipitated sample at ambient temperature and at $T = 190$ K. Curiously, the 4-^{13}C signal is not observed at ambient temperature while for the same sample at 190 K the 4-^{13}C signal is clearly visible. In order to investigate whether the loss of NMR signal coincides with the freezing transition of the entire sample, we have

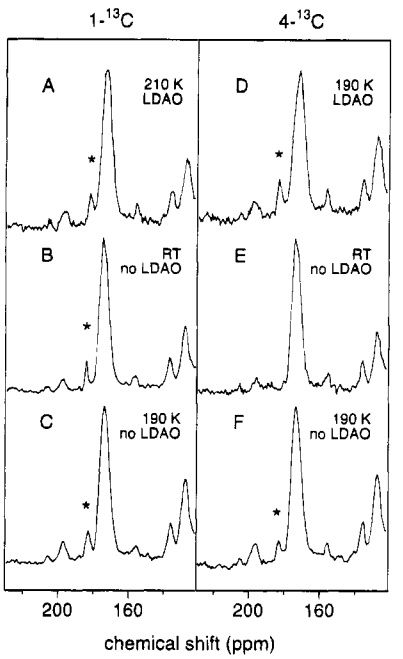

FIGURE 3: Aromatic and carbonylic regions of the proton-decoupled ^{13}C CP/MAS spectra of *Rb. sphaeroides* R26 RC, reconstituted with [1-^{13}C]UQ_{10} (A−C) or [4-^{13}C]UQ_{10} (D−F) at the Q_A site. In A and D the data for the frozen detergent-solubilized samples are shown, at $T = 210$ K and $T = 190$ K, respectively. The room temperature response from the precipitated samples is plotted in B and E, while C and F contain data for the same samples after cooling to $T = 190$ K. The center band response of the label in each dataset is indicated with an asterisk.

recorded series of 4-^{13}C Q_A spectra for two independently prepared samples, solubilized in detergent or precipitated, down to temperatures of 170 K (data not shown). For all preparations the [4-^{13}C]Q_A signal was observed only at temperatures $T \leq 255$ K. For the detergent-solubilized samples this is significantly lower than the freezing point of the entire sample, T ~265 K.

To determine if the 4-^{13}C signal at ambient temperature is shifted to a different spectral region, for instance ~173 ppm, the keto carbon shift observed for naphtazarine, in the presence of an intramolecular resonating hydrogen bond, the 140−160 ppm range typical for a hydroquinone hydroxy carbon, or as a remote and extreme possibility, the 90−110 ppm range, where an acetal-, or ketal-type ^{13}C nucleus is expected to resonate (Kalinowski et al., 1988), difference spectroscopy was performed to separate the signals from the labels from the protein background. Figure 4 shows the result of such a difference experiment (Figure 4C) from a 4-^{13}C (Figure 4A) and a 3-$^{13}CH_3$ (Figure 4B) Q_A sample. Both datasets were collected at room temperature with a spinning speed $\omega_r/2\pi = 7.00$ kHz. The difference spectrum for these two labels contains a strong negative signal from the 3-$^{13}CH_3$ label at 11.5 ppm (Figure 4C). There appears no positive signal of comparable intensity that could originate from the 4-^{13}C position.

In contrast with the 4-^{13}C, the positions 1, 2, and 3 all give good difference spectra at ambient temperature, yielding clear signals for the labeled positions. For the precipitated samples, the temperature dependence of the signals from these other labels is only weak and for detergent-solubilized samples the NMR response is "normal", i.e., the signals of the labels can be observed at any temperature below the freezing point of the sample. The resonances of the labels

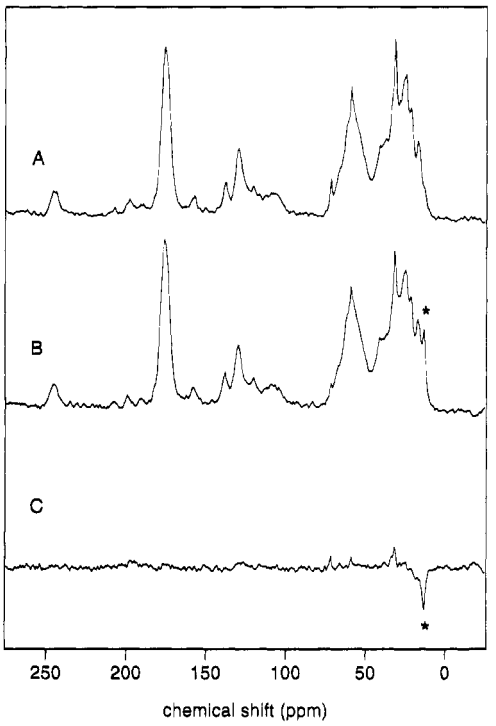

FIGURE 4: Proton-decoupled ^{13}C CP/MAS difference spectroscopy. Spectrum of precipitated *Rb. sphaeroides* R26 RCs at ambient temperature with $\omega_r/2\pi$ = 7.00 kHz. (A) Reconstituted with [4-^{13}C]UQ_{10} in the Q_A site and (B) reconstituted with [3-$^{13}CH_3$]UQ_{10} in the Q_A site. (C) 4-^{13}C minus 3-$^{13}CH_3$ difference spectrum. The three small positive signals at 31, 58, and 71 ppm, originate from a slight difference in residual LDAO detergent concentration between the two samples (cf. Fischer et al., 1992).

in Q_A broaden slightly by ~50 Hz upon cooling, and the observed line widths compare well with those found for solid UQ_{10} (cf. Table 1). The chemical shifts are almost independent of temperature. Carbonyl 1 shifts 2 ppm upfield when cooling to 190 K, while the signals from positions 2 and 3 shift upfield by 0.5 ppm when cooling to 230 and 190 K, respectively.

Next, we have investigated the variation of the cross-polarization efficiency for both carbonyls. Series of low-temperature data were collected at different τ_{cp} for detergent solubilized samples of [1-^{13}C]Q_A and [4-^{13}C]Q_A reconstituted RCs. For every spectrum the region from 190 to 160 ppm was deconvoluted with a superposition of two Gaussian lines, one for the response of the label at 183.8 (1-^{13}C) or 183.1 ppm (4-^{13}C) and another one for the strong peptide natural abundance background signal at 173 ppm. For both samples the carbonyl region of a dataset collected with τ_{cp} = 5 ms, near to the CP optimum, was first deconvoluted and the integrated intensities, and the line widths and the chemical shifts of the two signals were determined. Subsequently, for each label the other spectra in the series with different τ_{cp} were analyzed while keeping the line widths and the chemical shifts fixed to their values at τ_{cp} = 5 ms. This leaves the integrated intensities of the label and the natural abundance carbonyl signal as the only two free parameters, and they can be determined with good accuracy.

The result of this analysis is summarized in Figure 5, where the intensities of both quinone carbonyl labels and the peptide carbonyl background signal are plotted against τ_{cp}. In order to compare the results for the two different samples, all intensities were normalized relative to the maxima of the peptide carbonyl responses. These data were fitted to the expression for the cross-polarization intensity $I(\tau_{cp})$ given in Materials and Methods. For the strong protein carbonyl signal $T_{1\varrho}^{H}$ ~4 ms, and T_{CH} ~0.5 ms. The relative intensities of positions 1 and 4 are roughly equal and, when fitted to the single biexponential expression for $I(\tau_{cp})$, yielded both $T_{1\varrho}^{H}$ ~4 ms and T_{CH} ~4 ms. The solid lines in Figure 5 are obtained with eq 1, using these fit parameters.

The same set of samples that was used for the difference spectroscopy at higher speeds was also used in a series of experiments at lower sample rotation rates. Although the complete set of samples was prepared from one single batch of RCs, minor variations between the NMR response from different samples is inevitable, as there are several preparation steps after the reconstitution with labeled UQ_{10}. In practice, the most convenient way to interpret the low-speed difference data is by simply taking the first or second derivative of the signal, which effectively supresses the baseline roll in favor of the narrow responses from the labels at the expense of signal-to-noise [see, e.g., McDermott et al. (1991)]. In the earlier MAS studies of site-specifically labeled bacterial RC, second derivatives of NMR signals collected at moderately high spinning speeds were used (Fischer et al., 1992; de Groot et al., 1992; Shochat et al., 1995). Since the Q_A lines are consistently broader than the signals from the labels that were of interest in these earlier studies, and most of the signal intensity is now in the side bands, the signal-to-noise of the second derivatives is rather poor, and first derivatives yield optimal results.

The first derivative of a 1-^{13}C minus 3-^{13}C Q_A difference spectrum, taken at room temperature with a spinning speed $\omega_r/2\pi$ = 3.00 kHz, is shown in Figure 6A. At this spinning speed multiple side bands are clearly visible for the 1-^{13}C signal with the center band at 183.8 ppm and for the 3-^{13}C signal with the center band at 137.2 ppm. Figure 6B depicts the first derivative of the 4-^{13}C minus 2-^{13}C Q_A difference spectrum. These data were collected at low temperature, T = 190 K, as the 4-^{13}C signal could not be observed at ambient temperature. From these derivative difference spectra, the anisotropy parameters δ and η of the chemical shift tensor have been estimated for the labeled positions by iterative fitting of the derivative of a superposition of MAS patterns generated with the full powder simulation routine of Munowitz and Griffin (1982) to the experimental data. The results are summarized in Table 1. In addition, the CP/MAS NMR spectra of UQ_{10}, labeled on positions 1, 2, 3, and 4 in solid UQ_{10} have been recorded, and the CSA information for these labels is included in Table 1.

Generally, quinhydrone complexes, stabilized by π-stacking and hydrogen-bond interactions [see, e.g., Sakurai, (1965)], are considered for modeling Q_A bonding interactions (Bauscher et al., 1993; Breton et al., 1994). For aliphatic carbonyl compounds changes in solvent polarity and hydrogen-bonding capability induce shifts for both the FTIR C=O stretch frequency (up to 28 cm^{-1}) *and* the NMR carbonyl signal (up to ~7 ppm; Hartwell et al., 1948; Maciel & Ruben, 1963; Maciel & Natterstad, 1965). However, quinones in solution are rather insensitive to the hydrogen-bonding capability of the solvent. For instance, for ubiquinone-0 we have measured the C=O shifts in CD_3CN and CD_3OH, and the difference is 1 ppm only, while the corresponding shift in FTIR C=O stretch vibration is also small (1 cm^{-1};

Table 1: ^{13}C Shifts σ_i and Estimated Anisotropy Parameters (δ, η) for the Labels in Ubiquinone-10, Pure (UQ_{10}), and in the Q_A Binding Site (Q_A)

	UQ_{10} solution[a]	UQ_{10} crystalline				Q_A			
label	σ_i (ppm)	σ_i (ppm)	FWHM (Hz)	δ (kHz)	η	σ_i (ppm)	FWHM (Hz)	δ (kHz)	η
1	183.9	183.6	190	−9.7	0.7	183.8	150	−11	0.6
2	141.7	142.6	220	−9.3	1.0	143.7	320	−10[a]	1.0[a]
3	138.8	138.3	350	−9.4	0.9	137.2	320	−11	0.7
4	184.7	184.2	320	−9.6	0.7	183.1[b]	220[a]	−10[a]	0.3
3-Me	11.8	11.3				11.5			

[a] $CDCl_3$. [b] The data for the [4-^{13}C] Q_A were collected at a temperature of 190 K; all other data were acquired at ambient temperature.

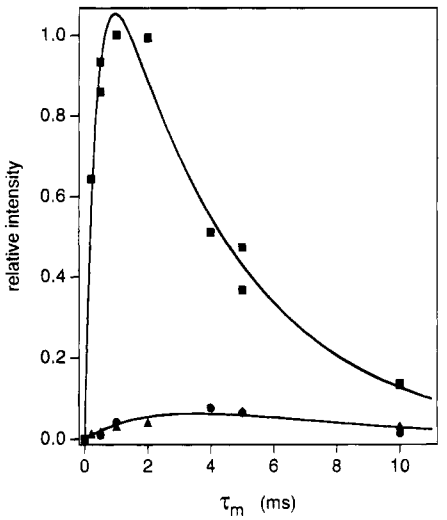

FIGURE 5: Integrated signal intensities of the protein peptide carbonyl signal (■), the [1-^{13}C]Q_A signal taken at T ~230 K (▲), and the 4-^{13}C Q_A signal at T ~190K (●) as a function of cross-polarization time τ_{cp}. The thick lines represent fits to the theoretical expression for $I(\tau_{cp})$.

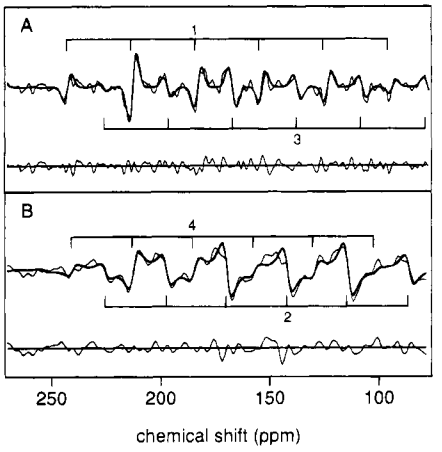

FIGURE 6: First derivatives of the 1-^{13}C minus 3-^{13}C (A) and the 4-^{13}C minus 2-^{13}C (B) difference spectra. The thin lines represent the data, and the solid line is a fit to the derivative of a superposition of MAS patterns. Below each derivative difference spectrum the residuals, data minus fit, are shown. Data for A were collected at ambient temperature with a spinning speed of $\omega_r/2\pi$ = 3.00 kHz, while the data for B were acquired at a low temperature T = 190 K with $\omega_r/2\pi$ = 2.80 kHz.

Bauscher & Mäntele, 1992). Hence, the effect of hydrogen bond donating capability on the C=O NMR signals in solution is minimal for ubiquinones. In order to parallel the earlier spectroscopic investigations of the Q_A, in particular those with FTIR, we have investigated the two quinhydrone complexes benzoquinone−hydroquinone and duroquinone−durohydroquinone and compared the results with data for

Table 2: ^{13}C Shifts σ_i and Anisotropy Parameters (δ, η) at Ambient Temperature for the Carbonyl and Olefinic Carbons in Benzoquinone Q_0, DQ_0, and the Q_0 or DQ_0 Quinone Entities in the Corresponding Quinhydrone Complex Formed with Benzoquinol and Duroquinol, Respectively

		quinone			quinhydrone complex		
	position	σ_i (ppm)	δ (kHz)	η	σ_i (ppm)	δ (kHz)	η
Q_0	C=O	189.0	−12.1	0.4	186.4	−12.2	0.0
	CH	137.0	10.7	0.8	136.4[a]	9.7	0.9
					134.1		
DQ_0	C=O	184.1	−11.2	0.6	184.8	−10.8	0.1
	CH	141.0	−10.7	1.0	140.5	−10.3	1.0

[a] The CH ^{13}C NMR response comprises two signals of approximate equal strength.

the corresponding quinones. Table 2 lists the chemical shift parameters for the ^{13}C NMR response of the ring carbons of both quinones and the quinone entities in the corresponding quinhydrone complexes. Estimated errors ($\pm\Delta$) for the solid UQ_{10}, Q_0, and DQ_0 data are $\Delta\sigma_i$ = 0.2 ppm, ΔFWHM = 20 Hz, $\Delta\delta$ = 0.4 kHz, and $\Delta\eta$ = 0.1. For the Q_A measurements $\Delta\sigma_i$ = 0.2 ppm, ΔFWHM = 30 Hz, $\Delta\delta$ = 1 kHz, and $\Delta\eta$ = 0.2.

DISCUSSION

A central and still open question in the characterization of the Q_A binding is the interaction with the protein environment at the carbonyl functionalities. Various molecular mechanisms for Q_A binding in photosynthetic reaction centers and for the origin of the asymmetry have been proposed. It is generally assumed that the binding of Q_A proceeds through strong interactions at one or both carbonyls (Bixon et al., 1991; Warncke & Dutton, 1993). In the charge-separated state one mode dominated by the 4-C−O vibration is characteristic for strong hydrogen bonding, but the ground-state shift of 60 cm^{-1} would imply a binding energy of −8 kcal/mol, which is too large to be explained in terms of a strong hydrogen bond interaction only (Brudler et al., 1994; Breton et al., 1994b). The mode dominated by the 1-C=O vibration is characteristic for an essentially free carbonyl group (Brudler et al, 1994; Breton et al., 1994b), while the available X-ray structures suggest the possibility for hydrogen bonding at carbonyl 1 with the peptide NH of Ala M260 (Allen et al., 1987; Chang et al., 1991; Ermler et al., 1994). In addition, similarities between the FTIR characteristics of Q_A and quinones in quinhydrone complexes stabilized by π-stacking interactions and hydrogen bonds have been noted (Bauscher et al., 1993; Brudler et al, 1994; Breton et al., 1994b), and site-directed mutagenesis studies on the Q_A binding site in the homologous *Rhodobacter capsulatus* RC were interpreted in terms of interactions between a highly conserved Trp residue and Q_A (Coleman et al., 1989a,b).

In this work we present the first ^{13}C NMR characterization of Q_A using site-specific labeling of positions 1, 2, 3, and 4 forming a path in the quinone ring between the two carbonyls (Figure 1). The protein−cofactor interactions affecting the quinone ring system can be investigated through the effects on the chemical shifts, the anisotropies, line widths, and cross-polarization efficiencies of the NMR response of the labels, providing another step toward a detailed characterization of Q_A binding in the RC.

^{13}C NMR Evidence for a Functionally Asymmetric Q_A Binding Pocket. The present study confirms asymmetric binding of Q_A by the protein. The most remarkable difference in NMR properties between the two carbonyl positions in Q_A is the temperature dependence of the signal at position 4, which is not detected at temperatures $T \geq 255$ K (cf. Figure 3). This temperature effect is now observed routinely in our laboratories, and its origin is currently being investigated in detail. It reproduces between samples as it has been detected for two independent RC preparations. It occurs both for RC solubilized with detergent and for RC precipitated from suspension. From the difference spectrum in Figure 4 it can be concluded that the signal is not shifted to another region of the spectrum while the comparison of the CP transfer characteristics in Figure 5 shows that the signal from the 1-^{13}C and 4-^{13}C labels are of comparable intensity at low temperatures.

Since the chemical shift is almost independent of temperature and there is no pronounced additional line broadening when the temperature is *lowered* from 255 to 180 K, the 4-^{13}C signal loss can not be attributed to dipolar interactions with the paramagnetic non-heme Fe^{2+}. In addition, the effect of an unpaired electronic spin in the vicinity of our label would shorten the $T_{1\varrho}^{H}$ of the surrounding at the lower temperatures, giving rise to shorter optimal CP times (Lowe & Tse, 1968; Devreux et al., 1973; Fischer et al., 1992). Since the correlation time of the $L = 2$, $S = 2$ Fe^{2+} electronic spin is expected to be in the range of $10^{-10}-10^{-12}$ s, very short compared to the NMR window of $10^{-5}-10^{-8}$ s, relaxation broadening or interference with the CP transfer originating from the Fe^{2+} paramagnetic center should become more pronounced when *cooling* the sample.

The differences in isotropic shifts between crystalline UQ_{10} and Q_A are only 0.2−1.1 ppm for the labeled positions. In contrast, recent FTIR experiments have revealed a ground-state shift of 60 cm^{-1} for a Q_A mode dominated by the 4-C=O vibration (Brudler et al.; 1994, Breton et al., 1994). In line with the NMR results for the 4-position of the Q_A, the isotropic shifts of the carbonyl signals in the two quinhydrone complexes are close to the ^{13}C=O shifts for the corresponding quinones, despite a substantial bond order change upon complex formation as was previously deduced from the 20−30 cm^{-1} shift of the carbonyl stretch frequencies (Slifkin & Walmsey, 1970; Kruk et al., 1993; Bauscher et al., 1993).

Even without substantial changes of the isotropic shift, variations of principal components of the chemical shift tensor can be quite large. For instance, for both quinhydrone complexes the carbonyl CSA is almost axially symmetric, $\eta \sim 0$, while for the corresponding and structurally more symmetric quinones $\eta \sim 0.5$ (cf. Table 2). A deconvolution analysis using computer-generated MAS patterns of the Q_A carbonyl data in Figure 6 indicates that the chemical shift asymmetry η for the 4-C=O is somewhat smaller than for the 4-position in crystalline UQ_{10} (cf. Table 1).

Unfortunately, calculation of the chemical shift anisotropy is not straightforward and impossible without exact knowledge of electronic distributions and underlying structure. In a highly simplified formalism the chemical shielding of atom A can be expressed as the sum of a paramagnetic and a diamagnetic term

$$\sigma = \sigma_d + \sigma_p \tag{2}$$

The diamagnetic shift σ_d depends on the relative placements of the atoms and the associated electron densities, while in this description the paramagnetic term σ_p takes into account the hybridization effects. In an average energy approximation, using a simple LCAO molecular orbital scheme (Pople, 1962),

$$\sigma_p^{zz} = -\frac{e^2\hbar^2}{2m^2c^2\Delta E}\langle r^{-3}\rangle(Q_{AA}^{zz} + \sum_{B\neq A} Q_{AB}^{zz}) \tag{3}$$

with e and m the charge and mass of the electron, $\hbar$ Planck's constant divided by 2π, c the velocity of light, and ΔE the average excitation energy of the excited electronic states in the absence of a magnetic field. The summation runs over neighbors B of A, the atom with the nucleus of interest, and σ_p is proportional to the average value $\langle r^{-3}\rangle$ for the 2p orbitals. Following Pople (1962), we write

$$Q_{AA}^{zz} = 2 - 2(P_{x_Ax_A} - 1)(P_{y_Ay_A} - 1) + 2P^2_{x_Ay_A} \tag{4}$$

$$Q_{AB}^{zz} = -2P_{x_Ax_B}P_{y_Ay_B} + 2P_{x_Ay_B}P_{y_Ax_B} \tag{5}$$

Similar expressions exist for σ_p^{xx} and σ_p^{yy}. The first part Q_{AA}^{zz} is expressed in terms of the generalized charge densities $P_{i_Aj_A}$, while the nearest neighbour bond effect Q_{AB}^{zz} is expressed in terms of the generalized bond orders $P_{i_Aj_B}$. Because of the ordering of the MO coefficients in the $P_{i_Aj_A}$ and the $P_{i_Aj_B}$, $\pi-\pi^*$ transitions are not contributing to the σ_p in this model (Pople, 1962). However, bond order changes may be expected to affect the principal components of the chemical shift tensor considerably through the terms that depend on $P_{i_Aj_B}$.

From experimental data for the relation between carbonyl frequencies and bond orders (Josien et al., 1953), it can be inferred that the 60 cm^{-1} shift of the mode dominated by the C=O stretch represents a variation of the bond order of approximately 0.1. A crude estimate based on trends put forward in a recent inventarisation of characteristic shielding anisotropies and approximate calculation of shielding tensors using eqs 3−5 suggests that σ_p contributions to the tensor elements could give rise to changes in the 10 ppm range for a bond order change of ~0.1 (Zilm & Duchamp, 1992). In addition, the σ_d can vary depending on the surrounding structure. However, with experimental errors in the range of 10−20 ppm, for the principal components of the chemical shift tensor for the Q_A carbonyls listed in Table 1, we conclude that there is at present no conflict between the NMR shift anisotropy analysis and the quite dramatic shift of the C=O stretch mode observed with infrared spectroscopy, as the latter technique is apparently much more sensitive to rehybridization effects. It is perhaps encouraging that our

estimates of the shift anisotropy indicate an effect at C-4 and not at C-1 (cf. Table 1), in line with the FTIR results.

Evidence for Dynamic Q_A−Protein Interactions Interfering with the NMR. The fact that a strong and narrow response for the 1-C=O can be detected at ambient temperature provides evidence that this carbonyl is static on the scale of the NMR and in a well-defined part of the binding pocket. On the other hand, the loss of 4-^{13}C signal for $T \geq 255$ K should be related to dynamic destructive interference of motion with CP efficiency, proton decoupling or MAS averaging. The C−H dipolar coupling frequency is typically in the 5 kHz range, proton decoupling is operating at ~50 kHz and MAS averaging uses $\omega_r/2\pi = 7$ kHz. The CP/MAS experiment is therefore sensitive to dynamic perturbations with correlation times in the 0.01−1 ms range, and in particular CP and decoupling are very sensitive to local dynamics. Recent additional experiments support these inferences and suggest that the temperature dependence of the 4-C=O signal is related to a shortening of the $T_{1\varrho}$ at temperatures approaching 255 K (B. J. van Rossum et al., unpublished results).

Several possible mechanisms for the temperature effects on the NMR signal have already been put forward in the literature (Brudler et al., 1994; Breton et al., 1994b). It could be related to dynamic hydrogen-bonding interactions on the scale of the NMR, 0.01−1 ms, for instance switching between the two possible hydrogen-bond donors. In such a scheme the dynamics would freeze at lower temperatures, explaining why for $T \geq 255$ K the 4-carbonyl signal can be observed. The available X-ray data suggest that carbonyl 4 of Q_A could form a hydrogen bond with His M219 or Thr M222 (Allen et al., 1987; Chang et al., 1991; Ermler et al., 1994). Kleinfeld et al. (1984) inferred that under physiological conditions transitions between different structural states occur on a time scale $\ll 10^{-1}$ s, affecting the P−Q_A distance by ~1 Å. In our opinion a mechanism involving dynamically shifting electron densities in a resonating hydrogen bonding environment, similar to the tautomeric equilibrium in naphtazarine, as suggested by Breton et al. (1994b), is unlikely. In this case a single shifted resonance is expected above the phase transition, which is not observed in our experiments (cf. Figure 4C). For instance, we have measured a chemical shift of 172.9 ppm for the 1-carbon in naphtazarine at ambient temperature when the molecule is in tautomeric equilibrium. Below the phase transition the intensity should be divided over two signals, while the comparison of the CP efficiency in Figure 5 suggests that the intensity of the 4-C=O signal at 183.1 ppm matches the intensity of the 1-C=O signal very well. Any explanation in terms of a precise molecular mechanism is at present speculative and further studies are necessary to resolve this point.

The Q_A Binding Site, As Probed by the Labels, Is Apolar. The differences in chemical shifts between Q_A and solid UQ_{10} are 0.2−1.1 ppm for the labeled positions. This amounts to polarizations of 0.02 electronic equivalent or less, as the charge of one electron produces a ^{13}C shift of ~160 ppm in an aromatic or olefinic system (Spiesecke & Schneider, 1961; Strub et al., 1983). Thus, our results show that the polarization of ubiquinone-10 by the protein surrounding in the Q_A site probed by the labels is minimal. This correlates well with the image of an apolar binding site transpiring from X-ray data (Allen et al., 1987; Chang et al., 1991; Ermler et al., 1994). In particular, the perturbation of the quinone ring responsible for the 60 cm^{-1} shift of the mode predominantly associated with the 4-C=O stretch (Brudler et al., 1994) does not give rise to a polarization of the 4-carbon on the scale of the NMR, since no additional shift of the 4-^{13}C signal in Q_A relative to solid UQ_{10} is observed.

The Q_A Site Is Heterogeneous on the Scale of the ^{13}C NMR. The observed line widths of our labeled positions are consistently in the 150−350 Hz range. This is comparable to what is observed for solid UQ_{10} but an order of magnitude broader than the 27 ± 5 Hz line width found for tyrosine M210, which resides in the immediate environment of the special pair (Fischer et al., 1992). The T_2 has been estimated from spin-echo experiments for both the 1-^{13}C and the 4-^{13}C labels, and it was found that homogeneous broadening can only account for half of the excess line width. Upon cooling, additional inhomogeneous broadening occurs for positions 1 and 2. This contrasts with the result obtained for the Tyr M 210 [4′-^{13}C] label, which gave the same line width between 170 and 250 K. This implies that the Q_A binding site is sensitive to the stress and strain exerted by the surrounding ice matrix and is more heterogeneous than, for instance, the almost crystalline environment of tyrosine M210, close to the special pair (Fischer et al., 1992; Shochat et al., 1995).

Conclusions. The NMR data reveal an apolar Q_A site, and there is no evidence for electrostatic polarization of the quinoid ring by a particularly strong binding interaction with the protein. The 4-^{13}C CSA of Q_A appears to be more symmetric than the CSA of the same label in solid UQ_{10}, while the 1-C=O in Q_A is essentially unperturbed. Considering the experimental errors for the principal components of the 4-^{13}C CSA, the NMR data are compatible with a pronounced decrease of the 4-C=O bond order upon binding to the protein. The Q_A binding site appears slightly heterogeneous on the scale of the NMR, and relative to other parts of the protein complex, in particular the environment of the special pair. The temperature dependence of the 4-^{13}C signal confirms the asymmetric binding of Q_A by the protein. As the CP efficiency decreases when the temperature approaches 255 K, the asymmetry is most likely related to a dynamic process at or close to the 4 carbonyl position interfering with the CP/MAS at physiological temperatures. The detailed characterization of this process requires an in-depth study with 1-D and 2-D NMR techniques at different temperatures.

ACKNOWLEDGMENT

We thank A. H. M. de Wit for culturing the cells and S. J. Jansen for isolating the reaction centers. K. Gerwert and J. Breton are gratefully acknowledged for extensive discussions on the different interpretations of FTIR and NMR spectroscopic results.

REFERENCES

Allen, P. J., Feher, G., Yeates, T. O., Komiya, H., & Rees, D. C. (1987) *Proc. Natl. Acad. Sci. U.S.A. 84*, 5730−5734.

Bauscher, M., & Mäntele, W. (1992) *J. Phys. Chem. 96*, 11101−11108.

Bauscher, M., Leonhard, M., Moss, D. A., & Mäntele, W. (1993) *Biochim. Biophys. Acta 1183*, 59−71.

Bixon, M., Fajer, G., Feher, J. H., Freed, J. H., Gamliel, G., Hoff, A. J., Levanon, H., Möbius, K., Nechustai, J. R., Norris, J. R.,

Schertz, J. L., Sessler, J. L., & Stehlik, D. (1991) *Isr. J. Chem. 32*−*4*, 369 ff.
Breton, J., Burie, J.-R., Berthomieu, C., Berger, G., & Nabedryk, E, (1994a) *Biochemistry 33*, 4953−4963.
Breton, J., Boullais, C., Burie, J.-R., Nabedryk, E., & Mioskowski, C. (1994b) *Biochemistry 33,* 14378−14386.
Brudler, R., de Groot, H. J. M., van Liemt, W. B. S., Steggerda, W. F., Esmeijer, R., Gast, P., Hoff, A. J., Lugtenburg, J., & Gerwert, K. (1994) *EMBO J. 13,* 5523−5530.
Chang, C.-H., El-Kabbani, O., Tiede, D., Norris, J., & Schiffer, M. (1991) *Biochemistry 30,* 5352−5360.
Coleman, W. J., Bylina, E. J., Youvan, D. C. (1989a) in *Current Research in Photosynthesis I* (Baltscheffsky, M.,Ed.) pp 149−152, Kluwer Academic Publishers, Dordrecht, The Netherlands.
Coleman, W. J., Youvan, D. C., Aumeier, W., Eberl, U., Volk, M., Lang, E., Siegl, J., Heckmann, R., Lersch, W., Ogrodnik, A., & Michel-Beyerle, M. E. (1989b) in *Current Research in Photosynthesis I* (Baltscheffsky, M., Ed.) pp 153−156, Kluwer Academic Publishers, Dordrecht, The Netherlands.
De Groot, H. J. M., Copié, V., Smith, S. O., Allen, P. J., Winkel, C., Lugtenburg, J., Herzfeld, J., & Griffin, R. G. (1988) *J. Magn. Reson. 77*, 251−257.
De Groot, H. J. M., Smith, S. O., Kolbert, A. C., Courtin, J. M. C., Winkel, C., Lugtenburg, J., Herzfeld, J., & Griffin, R. G (1991) *J. Magn. Reson. 91*, 30−38.
De Groot, H. J. M., Gebhard, R., van der Hoef, I., Hoff, A. J., Lugtenburg, J., Violette, C., & Frank, H. A. (1992) *Biochemistry 31,* 12446−12450.
Devreux, F., Boucher, J. P., & Nechtstein, M. (1973) *J. Phys. (Paris) 35*, 271−285.
Ermler, U., Fritzsch, G., Buchanan, S., & Michel, H. (1994) *Structure 2*, 925−936.
Feher, G., & Okamura, M. Y. (1978) in *The Photosynthetic Bacteria* (Clayton, R. K., & and Sistrom, W. R., Eds.) pp 349−386, Plenum Press, New York.
Feher, G., Isaacson, R. A., Okamura, M. Y., & Lubitz, W. (1985) in *Antennas and Reaction Centers of Photosynthetic Bacteria* (Michel-Beyerle, M.-E., Ed.) pp 174−189, Springer, Berlin.
Fischer, M. R., de Groot, H. J. M., Raap, J., Winkel, C., Hoff, A. J., & Lugtenburg, J. (1992) *Biochemistry 31*, 11038−11049.
Gast, P., Hemelrijk, P., & Hoff, A. J. (1994) *FEBS Lett. 337*, 39−42.
Gunner, M. R., Braun, B. S., Bruce, J. M., & Dutton, P. L. (1985) in *Antennas and Reaction Centers of Photosynthetic Bacteria* (Michel-Beyerle, M.-E., Ed.) pp 298−305, Springer, Berlin.
Josien, M.-L., Fuson, N., Lebas, J.-M., & Gregory, T. M. (1953) *J. Chem. Phys. 21*, 331−340.
Hartwell, E. J., Richards, R. E., & Thompson, H. W. (1948) *J. Chem. Soc.*, 1436−1441.
Hellingwerf, K. J. (1987) *J. Bioenerg. Biomembr. 19*, 203−223.
Herzfeld, J., & Berger, E. A. (1980) *J. Chem. Phys. 73*, 6021−6030.
Josien, M.-L., Fuson, N., Lebas, J.-M., & Gregory, T. M. (1953) *J. Chem. Phys. 21,* 331−340.
Kalinowski, H.-O., Berger, S., & Braun, S., (1988) in "*Carbon-13 NMR Spectroscopy*", pp 189, 306−330, Wiley and Sons, Chichester, U.K.
Kempf, J., Spiess, H. W., Haeberlen, U., & Zimmermann, K. (1974) *Chem. Phys. 4,* 269−276.
Kleinfeld, D., Okamura, M. Y., & Feher, G. (1984) *Biochemistry 23*, 5780−5786.
Kruk, J., Strzalka, K., & Leblanc, R. M. (1993) *Biophys. Chem. 45*, 235−244.
Lowe, I. J., & Tse, D. (1968) *Phys Rev. 166*, 279−291.
Lubitz, W., Abresch, E. C., Debus, R. J., Isaacson, R. A., Okamura, M. Y., & Feher, G. (1985) *Biochim. Biophys. Acta 808*, 464−469.
Maciel, G. E., & Ruben, G. C. (1963) *J. Am. Chem. Soc. 85*, 3903−3904.
Maciel, G. E., & Natterstad, J. J. (1965) *J. Chem. Phys. 42*−*8*, 2752−2759.
McDermott, A. E., Thompson, L. K., Winkel, C., Farrar, M. R., Pelletier, S., Lugtenburg, J., Herzfeld, J., & Griffin, R. G. (1991) *Biochemistry 30*, 8366−8371.
Mehring, M. (1983) in *Principles of High Resolution NMR in Solids*, p 151, Springer-Verlag, Berlin.
Morrison, L. E., Schelhorn, J. E., Cotton, T. M., Bering, C. L., & Loach, P. A. (1982) in *Function of Quinones in Energy Conserving Systems* (Trumpower, B. L., Ed.) pp 35−58, Academic Press, New York.
Munowitz, M. G., & Griffin, R. G. (1982) *J. Chem. Phys. 77*, 2217−2224.
Okamura, M. Y., Isaacson, R. A., & Feher, G. (1975) *Proc. Natl. Acad. Sci. U.S.A. 72*, 3491−3495.
Peersen, O., Wu, X., Kustanovich, I., & Smith, S. O. (1993) *J. Magn. Reson. A 104*, 334−339.
Pople, J. A. (1962) *J. Chem. Phys. 37,* 53−59.
Rees, D. C., Komiya, H., Yeates, T. O., Allen, J. P., & Feher, G. (1989) *Annu. Rev. Biochem. 58*, 607−663.
Sakurai, T. (1965) *Acta Crystallogr. 19*, 320−330.
Slifkin, M. A., & Walmsley, R. H. (1970) *Spectrochim. Acta 26A*, 1237−1242.
Shochat, S., Gast, P., Hoff, A. J., Boender, G. J., van Leeuwen, S., van Liemt, W. B. S., Vijgenboom, E., Raap, J., Lugtenburg, J., & de Groot, H. J. M. (1995) *Spectrochim. Acta 51A*, 135−144.
Slooten, L. (1972) *Biochim. Biophys. Acta 275*, 208−218.
Spiesecke, H., & Schneider, W. G. (1961) *Tetrahedron Lett. 2*, 468−472.
Strub, H., Beeler, A. J., Grant, D. M., Michl, J., Cutts, P. W., & Zilm, K. (1983) *J. Am. Chem. Soc. 105*, 3333−3334.
Van den Brink, J., Spolyakov, A., Van Liemt, W. B. S., Raap, J., Lugtenburg. J., Gast, P., & Hoff, A. J. (1994) *FEBS Lett. 353*, 273−276.
Van Liemt, W. B. S., Steggerda, W. F., Esmeijer, R., & Lugtenburg, J. (1994) *Recl. Trav. Chim. Pays-Bas 113*, 153−161.
Verméglio, A. (1982) in *Function of Quinones in Energy Conserving Systems* (Trumpower, B. L., Ed.) pp 169−179, Academic Press, New York.
Warncke, K., & Dutton, P. L., (1993) *Proc. Natl. Acad. Sci. U.S.A. 90*, 2920−2924.
Wraight, C. A. (1979) *Biochim. Biophys. Acta 548*, 309−327.
Zilm, K. W., & Duchamp, J. C., (1992) in *Nuclear Magnetic Shieldings and Molecular Structure* (Tossel, J. A., Ed.) pp 315−334, NATO ASI Series, Series C:, Mathematical and Physical Sciences, Springer, New York.

BI950029T